Talanta 216 (2020) 120913

Contents lists available at ScienceDirect

Talanta

journal homepage: www.elsevier.com/locate/talanta

Colorimetric detection of miRNA-21 by DNAzyme-coupled branched DNA constructs

Elyas Hosseinzadeh[a], Hadi Ravan[b,*], Abbas Mohammadi[a], Hossein Pourghadamyari[c,d,**]

[a] Sirjan School of Medical Sciences, Sirjan, Iran
[b] Department of Biology, Faculty of Sciences, Shahid Bahonar University of Kerman, Kerman, Iran
[c] Student Research Committee, Kerman University of Medical Sciences, Kerman, Iran
[d] Department of Clinical Biochemistry, Afzalipour School of Medicine, Kerman University of Medical Sciences, Iran

ARTICLE INFO

Keywords:
Strand displacement
Enzyme-free
Self-assembly
Nanostructures
Biosensor

ABSTRACT

Fluctuation of nucleic acid expression and ultrasensitive and specific detection of these variations in expression is a crucial subject in molecular medicine and clinical theranostics. A novel DNAzyme-coupled branched hybridization chain reaction (b-HCR) assay is reported for efficient signal-amplified detection of miRNA in this study. This assay was composed of a translator (T) hybridized with miR-21 to initiate the first HCR by hairpin 1 (H_1) and hairpin 2 (H_2). The primary HCR provided a backbone chain for numerous branches budding through hairpin 3 (H_3) and hairpin 4 (H_4) assembles. In the presence of hemin, the G-rich domains embedded in H1 and H4 produce an active G-quadruplex DNAzyme upon exposure to a target that could catalyze the oxidation of colorless substrate to colored product. The present approach has the potential to be used for quantitative detection of miR-21 with a sensitivity and a dynamic range of 1 pM and 1 pM to 1 nM, respectively.

1. Introduction

Dynamic DNA nanotechn, the science of DNA strand displacement reaction engineering, is utilized to construct molecular machines [1], enzyme-free catalytic systems [2–4] DNA chemical oscillators [5], and complex molecular computers [6–8]. This research field is used to control spatial and temporal distributions of DNA structures through various inducers, such as pH, ions, light, and protein/nucleic acid triggers [9–12]. Nucleic acid-dependent amplification methods, in particular those based on DNA strand displacement reaction, carry out expanding duties in different conditions of in vitro [13] and in vivo [14] as well as in artificial gene regulations [12]. Non-enzymatic catalytic devices based on strand displacement are nanomachines which can function as detectors or sensors of different analytes applied in chemistry and medical diagnostics. The function of these nanodevices is mediated by single stranded overhang (known as toehold) of pre-tailored hairpin monomers/linear multiplexes [2,3] that make them thermodynamically metastable for cross-opening via the toehold-mediated strand displacement (TMSD) reaction, to create thermodynamically more stable nanostructures. Hybridization chain reaction (HCR) [4], entropy-driven catalysis (EDC) [2], catalyzed hairpin assembly (CHA) [3], and cascade hybridization reaction (CHR) [14] are the most common TMSD-directed dynamical systems introduced in the past decades to be used in theranostic, biomaterial, data processing and transforming input molecules into readable signal output [15].

Originally developed by Dirks and Pierce [4], HCR is based on toehold-mediated strand invasion into stable hairpin structures. Two species of kinetically trapped metastable fuels accomplish the roles of recognition and signal amplification simultaneously upon the introduction of a trigger strand to assemble nicked polymeric double helices (DNA concatemers). Several subsequent investigators used this elegant principle in different systems with some modifications to improve its sensitivity, specificity, and application. For example, Willner's group was the first to combine different split-DNAzyme with HCR to enhance DNA detection sensitivity [16]. In a similar work, Dong et al. designed intact DNAzyme-locked hairpin probes to detect DNA and RNA by the colorimetric and fluorometric methods [17]. Choi et al. used HCR probes to simultaneously analyze different mRNAs in fixed zebrafish embryos by in situ HCR technology [18]. In another technique, Yang et al. developed HCR-integrated graphene oxide fluorescence switch-based assay for sensitive, specific and simple detection of miRNAs [19]. Moreover, Liao et al. developed dual signal amplification by combination of CHA and HCR to detect miRNAs in electrochemical and electrochemiluminescence (ECL)-based signal read out [20]. Beside

* Corresponding author. Department of Biology, Faculty of Sciences, Shahid Bahonar University of Kerman, Kerman, Iran.
** Corresponding author. Department of Clinical Biochemistry, Afzalipour School of Medicine, Kerman University of Medical Sciences, Iran.
E-mail addresses: ravan@uk.ac.ir (H. Ravan), ghadamyarih91@gmail.com (H. Pourghadamyari).

https://doi.org/10.1016/j.talanta.2020.120913
Received 2 December 2019; Received in revised form 18 February 2020; Accepted 8 March 2020
Available online 21 March 2020
0039-9140/

their action as biosensor for the detection of bioanalytes and cancer cells [21,22], HCR applications have recently attracted increasing attention for in situ and in vivo mapping of mRNAs [23], constructing complex nanostructures, drug delivery, and DNA hydrogels [24].

Linear growth of DNA concatemers in response to a trigger molecule is the rational mechanism in most cases of HCR; nonetheless, their limited efficiency in signal amplification because of chain-like reactions have motivated researchers to develop new HCR circuits with branched or nonlinear reactions. For example, Yin et al. [3] and Chandran et al. [25], independently, used hairpin monomers to develop HCRs with dendritic growth strategies; however, requirement of new hairpin species for each generation of dendritic growth in the first strategy and temperature changes during the reaction (non-isothermal), system leakage, and linear growth rather than dendritic growth in the later strategy, limited their broad application in DNA nanotechnology. Hsing's group developed dendritic DNA nanostructure producing procedures in different signal readout assays (electrochemical and fluorescence based) by employing double-stranded substrates to carry out nonlinear HCR. However, systems needed removing of the excess unreacted single stranded DNAs which complicated the strategies [26,27]. Tang et al. developed ligation mediated branched HCR to detect single nucleotide mutation in mRNA in fixed cells, but multi-step reactions and washing procedures make it complicated, time-consuming, and a not so user-friendly strategy [28]. Recently, Wei et al. developed a complex strategy of coupled HCR to detect miRNA in serum and living cells by fluorescence resonance energy transfer (FRET) technology [29]. In a similar work, Jiang and coworkers developed branched-HCR for efficient signal-amplified imaging of mRNA in living cells by fluorescent signal read out [23].

Here, an innovative DNAzyme integrated branched HCR (b-HCR) circuit with synergistic amplification performance is introduced (Scheme 1), which operates as the simplest model for homogeneous assay in a single reaction tube. The present two layered isothermal, non-enzymatic, and combinatory signal amplification system relies on a hierarchical coupling design of two DNAzyme-locked HCR circuits for efficient signal-amplified detection of miR-21, a short 22 nucleotides RNA molecule, which is overexpressed in several disease, particularly in different cancers [30,31]. Hence, a set of five DNA hairpins, including a translator/trigger (T), two monomer hairpins H_1 and H_2 for primary HCR, and two monomers H_3 and H_4 for secondary HCR were designed. The amplicon product of the primary HCR as a backbone for running the secondary HCR created a branched long dsDNA nanowire, and the DNAzyme moiety in this approach acted as the signal reporter exhibiting peroxidase-like activity in the presence of hemin, which unlike the splitting-DNAzyme, works based on intact G-quadruplex sequence linked to hairpin probes of b-HCR. Overall, with the proposed approach working with strong noise reduction, our design measured as low as 1 pM miR-21 with a linear range of 1 pM to 1 nM. Besides, the current approach showed excellent selectivity toward the perfect analogue of miR-21 against other single mismatched analogues.

2. Experimental section

2.1. Materials and reagents

All oligonucleotides were designed and then synthesized by Bioneer Co. (South Korea). They were HPLC- or PAGE-purified and freeze-dried by the company, used as provided and diluted in 10 mM phosphate buffer (PB, pH 7.0). The sequence of oligonucleotides is shown in Table 1. ABTS (2, 2-azino-bis, 3-ethylbenzothiazoline-6-sulfonic acid), Hemin, 4-(2-hydroxyethyl)-1- piperazineethane sulfonic acid (HEPES) and dimethyl sulfoxide (DMSO) were purchased from Sigma-Aldrich Co. (USA). Hemin stock solution (0.1 mM) was prepared in DMSO and stored in a dark bottle at −20 °C until needed. All aqueous solutions were prepared using ultrapure water passed through a Millipore Milli-Q water purification system with an electric resistance of 18.25 ($M\Omega\ cm^{-1}$).

§Segments marked with * are complementary to the corresponding unmarked segments. The underlined segment in H_1 and H_4 (g_1, g_2, g_3) strand represents peroxidase mimicking G-quadraplex DNAzyme. MS, MD, and MI oligonucleotides have the identical sequence as miR-21 except for single nucleotide substitution, deletion and insertion in gray background, respectively.

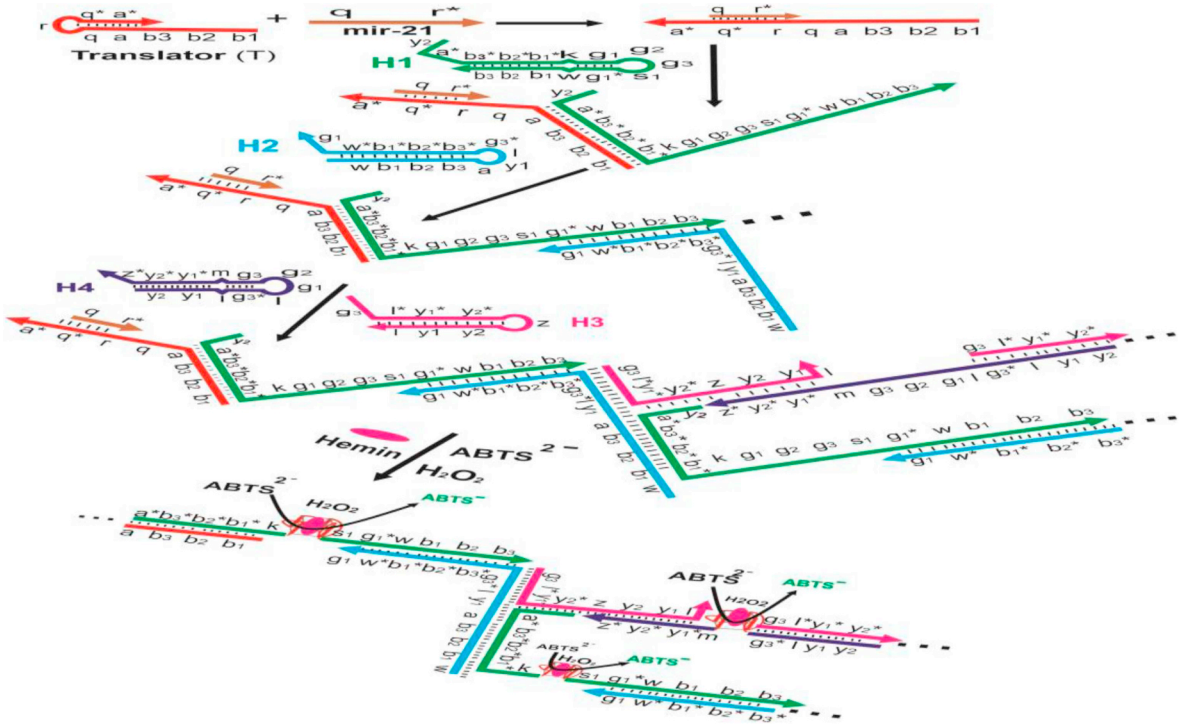

Scheme 1. Working principle of designed nanodevice by miR-21.

Table 1
Domains and sequences of the DNA oligonucleotides designed in the present study.

Oligonucleotide name	Sequence (5′-3′)	domains§
T	T▪G▪ACTTTACTTACTTTGC▪ATGATG▪TAGCTTATC▪TCAACATCAGTCT▪GATAAGCTA▪CATCAT	B_1▪b_2▪b_3▪a▪q▪r▪q*▪a*
H_1	CACCTCCACTTTCA▪CATCAT▪GCAAAGTAAGTAAAGT▪C▪A▪A▪TGGGTA▪ GGGCGGGTT▪GGGAAA▪G▪TACCCA▪G▪T▪G▪ACTTTACTTACTTTGC	y_2▪a*▪b_3*▪b_2*▪b_1*▪k▪g_1▪g_2▪g_3▪s▪g_1*▪w▪b_1▪b_2▪b_3
H_2	G▪T▪G▪ACTTTACTTACTTTGC▪ATGATG▪TCAC▪G▪TTTCCC▪ GCAAAGTAAGTAAAGT▪C▪A▪C▪TGGGTA	w▪b_1▪b_2▪b_3▪a▪y_1▪l▪g_3*▪b_3*▪b_2*▪b_1*▪w*▪g_1
H_3	GGGAAA▪C▪GTGA▪TGAAAGTGGAGGTG▪CCACTC▪CACCTCCACTTTCA▪TCAC▪G	g_3▪l*▪y_1*▪y_2*▪z▪y_2▪y_1▪l
H_4	CACCTCCACTTTCA▪TCAC▪G▪TTTCCC▪G▪TGGGTA▪GGGCGGGTT▪GGGAAA▪G▪GTGA▪ TGAAAGTGGAGGTG▪GAGTGG	y_2▪y_1▪l▪g_3*▪l▪g_1▪g_2▪g_3▪m▪yl*▪y_2*▪z*
miR-21	UAGCUUAUC▪AGACUGAUGUUGA	q▪r*
miR-21 sub (MS)	UAGCUUAgC▪AGACUGAUGUUGA	q▪r*
miR-21 del (MD)	UAGCUUA_C▪AGACUGAUGUUGA	q▪r*
miR-21 ins (MI)	UAGCUUAUgC▪AGACUGAUGUUGA	q▪r*

2.2. Target stimulated b-HCR assay confirmation by gel electrophoresis

The assay experiment was carried out in 15-μL hybridization buffer containing 1.2 μM of (T,H_1,H_2,H_3, and H_4), and 1 μM miR-21. Before mixing the reagents, all oligonucleotides were separately diluted to desired concentrations and incubated at 95° C for 5 min and allowed to cool down slowly to room temperature (RT). Then, the different solutions were mixed and incubated in RT for 2.5 h. Formation of the branched DNA nanostructure was checked by electrophoresis in a 2% agarose gel using cold Tris-acetate-EDTA buffer at a constant voltage of 80 V for 120 min. The ethidium bromide stained gel was visualized using UV-Doc HD 6 light box.

2.3. Colorimetric detection of miR-21

To avoid limitation of certain analytes, researchers designed particular oligonucleotide sequence, known as translator, with two unrelated DNA fragments, one fragment as a recognition element and the other as a universal reporter element, to convert different input analytes like nucleic acids and proteins, to the universal nucleic acid output [7,32,33]. In the present study we used a hairpin translator to convert miRNA to DNA strand to overcome miRNA drawbacks including small size and low stability according the previous work [20]. In that line, 50 μL of the T strand (1.2 μM) was added and then different concentrations of miR-21 (50 μL) were added to the microwells and incubated for 45 min at room temperature. During incubation time, miR-21 opened stem-loop structure of the T strand through TMSD and changed to active form. Ten μL of each hairpin monomer (H_1, H_2, H_3, H_4) with the final concentrations of 1.2 μM were added to the microwells' content, and incubated at 25 °C for 2 h. A solution containing 25 mM HEPES, 20 mM KCl, 200 mM NaCl, 0.5 μM hemin, 0.05% Triton X-100, and 1% DMSO was added to the microwells and incubated for 30 min at room temperature [22]. To this solution, 100 μL peroxidase substrate (2 mM H_2O_2 and 2 mM ABTS) was added, incubated for 20 min, and the absorbance was measured using a BioTek microtiter plate reader [34].

3. Results and discussion

3.1. Assay design and working principle

To obtain the highest signal, it is necessary to resolve some limitations belonging to miRNA properties like small size and low stability. Translating RNA to an arbitrary DNA or conversion to a complementary DNA, utilizing other complementary analogues like PNA and LNA, and utilizing phosphorothioate oligonucleotide are examples of the previously reported strategies to address these issues [33]. Of them, translation to the arbitrary DNA analogues can resolve both problems of miRNA and, because of its universal characteristic, can be used for the detection of various target molecules.

As shown in Scheme 1, five types of hairpin monomers were designed, which are metastable and can coexist in a single reaction tube until triggered by the initiator. The first hairpin (T), has two functional domains, one for recognition of miR-21 and the other for initiating amplification machine of the first HCR. The toehold region of the latter domain is concealed in the stem region of the T strand and will be exposed to the complementary sequence only after hybridization with miR-21. The fuels of the first HCR (H_1 and H_2), which act as the backbone for the second HCR, carry toehold domains at their 5′ and 3′ ends, respectively. The sequences of the H_1 and H_2 hairpins have been designed ingeniously, in which the sequences in the stem region of both hairpins were identical, the complementary sequence of H_1 toehold placed in the loop region of H_2 whereas, the H_1 loop was complementary to the H_2 toehold. (The sequences of H_3 and H_4 monomers were also designed in a similar way). Besides, H_1 and H_2 contain split initiator fragments for the secondary HCR in their toehold and loop regions, respectively. As the first HCR assembles in response to the translator, released by miR-21, these split initiator fragments come into close proximity, interact with H_3 toehold, and unfold the H_3 monomer for running the secondary HCR circuit in the presence of H_4. The bottom-up nucleation cascade of the hairpin monomers arranged the primary and the secondary HCR circuits, leads to the generation of a brush-like assembly in response to miR-21 as the earliest initiator. In detail, when monomers H_1 and H_2 unfolded in successive cross-opening reactions in response to T, some domains of these hairpins got closer due to the hairpin structure opening. In this situation, newly exposed single stranded parts of H_1 and H_2 acted as initiator fragments to trigger secondary HCR through chain-like nucleation between hairpin monomers H_3 and H_4. During the period of branched nanowires growing, DNAzyme-modified hairpins (H_1 and H_4) created an open but inactive DNAzyme. This DNAzyme transformed to its active configuration in the presence of hemin and potassium ions and converted colorless $ABTS^{2-}$ (2, 2-azino-bis, 3-ethylbenzothiazoline-6-sulfonic acid) to green $ABTS^{-}$. Briefly, the hairpin monomers of H_1 and H_4 were designed since they have G-quadraplex-DNAzyme sequences at stem and loop regions. One-third of the catalytic G-quadraplex (g_1, 6 nt) was concealed in the stem and two-thirds (g_2, 9 nt; g_3, 6 nt) in the loop regions of H_1 and H_4. In the absence of a target molecule, H_1 and H_4 were in closed hairpin state and the DNAzyme was in an inactive form. However, when the target was introduced, both hairpins exposed their sequestered sequences and created a full-length G-quadraplex DNAzyme, which, at the presence of hemin, changed to the active form. The activated DNAzyme converted a colorless substrate to a greenish product which would be detected in 415 nm. It is worthy pointing out that incorporation of split initiator fragments in the separate places, toehold region of H_1 monomer and loop region of H_2 monomer, restricted their reaction with H_3 toehold and triggering downstream HCR activation. In this sense, it is obvious that, in the absence of target trigger, the primary

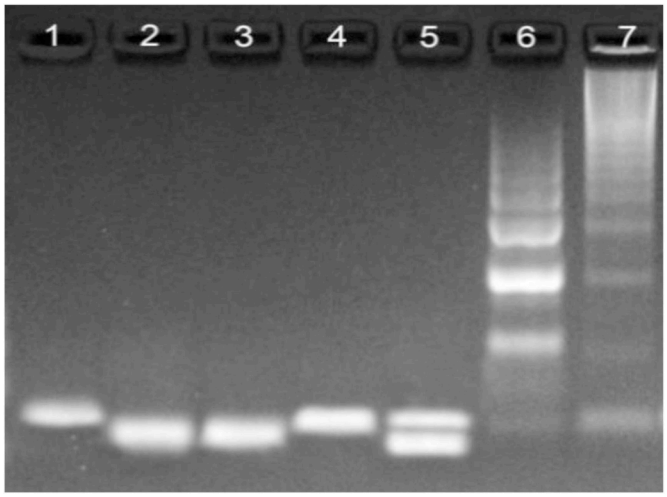

Fig. 1. Gel electrophoresis analysis of bHCR: lane 1, 1.2 μM H1; lane 2, 1.2 μM H2; lane 3, 1.2 μM H3; lane 4, 1.2 μM H4; lane 5, 1.2 μM T + 1.2 μM H1–H4; lane 6, 1 μM miR-21, 1.2 μM T, 1.2 μM H1 and 1.2 μM H2; lane 7, 1 μM miR-21, 1.2 μM T and 1.2 μM H1–H4.

and particularly the secondary HCRs were blocked; hence no branched assemblies were constructed and consequently the background signal was eliminated.

3.2. B-HCR mechanism demonstration by gel electrophoresis

To investigate if our hairpin monomers operate as expected, agarose gel electrophoresis was performed under optimized condition. As illustrated in Fig. 1, a single band corresponding to the hairpin monomers was observed in lanes 1–4. Identical bands in the same positions with no product were obtained in lane 5, where the upper band corresponds to H_1 and H_4, and the lower band corresponded to T, H_2 and H_3, suggesting sufficient stability of hairpin monomers to coexist in the absence of a trigger and as such, indicating that the DNA nanodevice did not operate nonspecifically to produce background bands. In contrast, ladder-like bands were observed in lane 6 upon addition of target trigger to H_1 and H_2 containing solution, characteristic of the first HCR circuit. In addition, split initiator fragments which mediated H_3 and then H_4 opening, leading to successive chain like reactions, were confirmed by different bands with obvious shift in the positions in the presence of target and H_1 to H_4 monomers in lane 7. As one can see, the corresponding monomer bands almost disappeared in lanes 6 and 7, indicating consumption of hairpin monomers and performance of the first and b-HCR in lanes 6 and 7, respectively. In view of this, the ladder pattern in lane 7 was different to those in lane 6 and also products with higher molecular weight in lane 7, this phenomenon clearly exhibits that the secondary HCR can be activated by the product of the first HCR and nucleated on them, strong convincing evidence for the reasonability of proposed DNA nanodevice.

3.3. Nanodevice target sensing feasibility

To further investigate the ability of the designed system to detect miRNA, different samples containing 1.2 μM of T and H1 to H4 were incubated with target miRNA and corresponding absorbance spectra were recorded. As displayed in Fig. 2a, in the absence of the trigger (miR-21), the absorbance spectra obtained from b-HCR containing 0.5 μM hemin solution, 1.2 μM T, and 1.2 μM H1 to H4 (curve b, blank) were similar to 0.5 μM hemin solution (curve a). This data clarify that the nonspecific reactions are diminished and background signal was minimized with our system. Interestingly, incubating the same reactants with 1 nM of miR-21, remarkably increased signal amplification, implying potential capability of this strategy for analyte detection. Incubation of target with first HCR fuels (0.5 μM hemin solution, 1.2 μM T, 1.2 μM H1 and H2, and 1 nM miR-21) increased signal amplification significantly (curve c) compared to the blank, but it was appreciably lower than the signal obtained from b-HCR containing (0.5 μM hemin solution, 1.2 μM T, and 1.2 μM H1 to H4) (curve d). As theoretically anticipated, in the absence of miR-21, there was no distinguishable signal related to hemin solution, furthermore, the individual first or the second HCR (data not shown) performance did not have enough efficiency to sense low abundance analytes like miRNA. The corresponding solution color changed under different conditions (Fig. 2b). According to confirmatory evidence obtained in this part, it is obvious that the developed nanodevice is a powerful system for target detecting.

3.4. Optimizing nanodevice experimental conditions

In order to eliminate the frustrating false-positive signal from b-HCR, all hairpins should remain in a sufficiently stable form in the absence of the initiator. Metastable hairpin monomers are the best form of oligonucleotide programing to diminish cross-reactions (leakage) between monomers and also between the first HCR and the second HCR until the target is introduced. To achieve this, toehold and/or binding regions of the output sequences of the primary HCR were designed to be inaccessible to prevent their probable interactions with each other and the secondary HCR before exposure. Controlling this phenomenon was checked theoretically and experimentally. Nevertheless, spontaneous opening of the monomer structures influenced by experimental conditions, such as concentration of hairpin monomers, temperature, and reaction time, is the inseparable part of all metastable fuels. To achieve the desirable results, parameters of temperature, time and reactants' concentrations were optimized. Initially, the hairpin monomers in b-HCR circuit reacted non-specifically even in the absence of target miRNA, with the increasing hairpin concentrations, background signal also increased. To reduce the prevalence of uncatalyzed reactions, various concentrations of the hairpin monomers ranging from 0.8 to 1.4 μM were examined. As seen in Fig. 3 a, the maximal value of signal was obtained at 1.2 μM, and further increasing the hairpin concentration would give lower signal as a result of high noise. Based on this result, 1.2 μM was selected as the optimal concentration of the hairpin monomers.

To further enhance the sensitivity, the duration and temperature for b-HCR performing was also optimized. Fig. 3b depicts the result of b-HCR incubating time in which the signal raised and reached the peak with the increase of incubation time up to 150 min; however, the signal to noise ratio tended to decrease at time intervals longer than 150 min by increasing uncatalyzed interactions between hairpins. Hence, this time was chosen as the optimal incubation time. Temperature can be considered a key factor to induce conformational changes of hairpin monomers leading to asymptotic leakage which is the primary source of system leak. At low temperatures, the hairpin monomers could not reach to a sufficient collision probability, while at high temperatures nonspecific reactions increased because the probability of hairpins' structure breathing increased [35–37]. With this in mind, the incubating temperature of proposed assay was optimized. As displayed in Fig. 3c, the peak value was obtained at 30 °C. Hence, 30 °C was determined as the optimum incubating temperature.

Initially, we explored cation effect on DNAzyme performance to achieve specific signal. Previous studies [38,39] have declared inevitable necessity of K^+ ions for the active folding of DNAzyme through inducing of guanine-rich DNAzymes to be in correct secondary and tertiary structure, capable of binding hemin. On this basis, we explored K^+ effect on DNAzyme activity at different concentrations (0–35 mM) KCl in a solution containing 25 mM HEPES, 200 mM NaCl, 0.5 μM hemin, 0.05% Triton X-100, and 1% DMSO. In conformity to the previous studies, increasing the cation concentration enhanced the

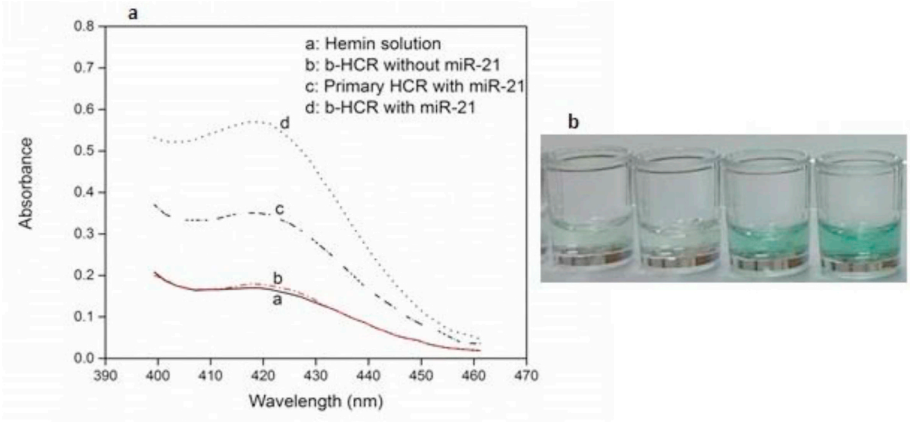

Fig. 2. Nanodevice ability for target sensing. a) Absorbance spectra for mixtures of (a) 0.5 μM hemin solution; (b) b-HCR in the presence of 0.5 μM hemin solution and 1.2 μM T, and 1.2 μM H1 to H4 (blank); (c) primary HCR in the presence of 0.5 μM hemin solution, 1.2 μM T, 1.2 μM H1 and H2, and 1 nM miR-21; (d) b-HCR in the presence of 0.5 μM hemin solution, 1.2 μM T, 1.2 μM H1 to H4, and 1 nM miR-21. b) Corresponding colors in respect to different conditions. (For interpretation of the references to color in this figure legend, the reader is referred to the Web version of this article.)

DNAzyme-catalyzed reaction, and the best response was obtained in 20 mM (Fig. 3d).

3.5. Nanodevice analytical performance

To confirm the nanodevice capability to detect the target molecule (miR-21), analytical performance of the assay was interrogated in advance. Fig. 4a indicates the spectral data of various target concentrations ranging from 0 to 3 nM. As anticipated, the signal was proportional to the concentration of target. The detection limit of the method was 1 pM, since at this concentration the target miRNA can induce a detectable signal based on 3σ rule (the threshold value is 0.22247). Fig. 4b shows calibration curve inferred from the absorbance values acquired at different concentrations, associated with a linear dynamic range (LDR) from 10 pM to 1 nM (Fig. 4c) with a correlation coefficient of 0.98 (Abs = 0.0003C + 0.2534). This finding was attributed to the fact of genius oligonucleotide designing and nonspecific reactions controlling. Several works have been reported with similar principle of action to analyze various targets. For example, Chandran et al. developed a dendritic based HCR for DNA detection as low as 10 nM by using semi-quantitative PAGE method [25]. Also, Bi and his coworkers developed branched HCR to detect target DNA with a detection limit of 0.1 pM and a dynamic range of 0.1 pM–1 nM using a fluorescence amplification technique [40]. This group also fabricated a combination strategy of CHA and HCR yielding hyper-branched DNA nanostructure to detect 0.72 pM target miRNA with a dynamic range of 1 pM–10 nM

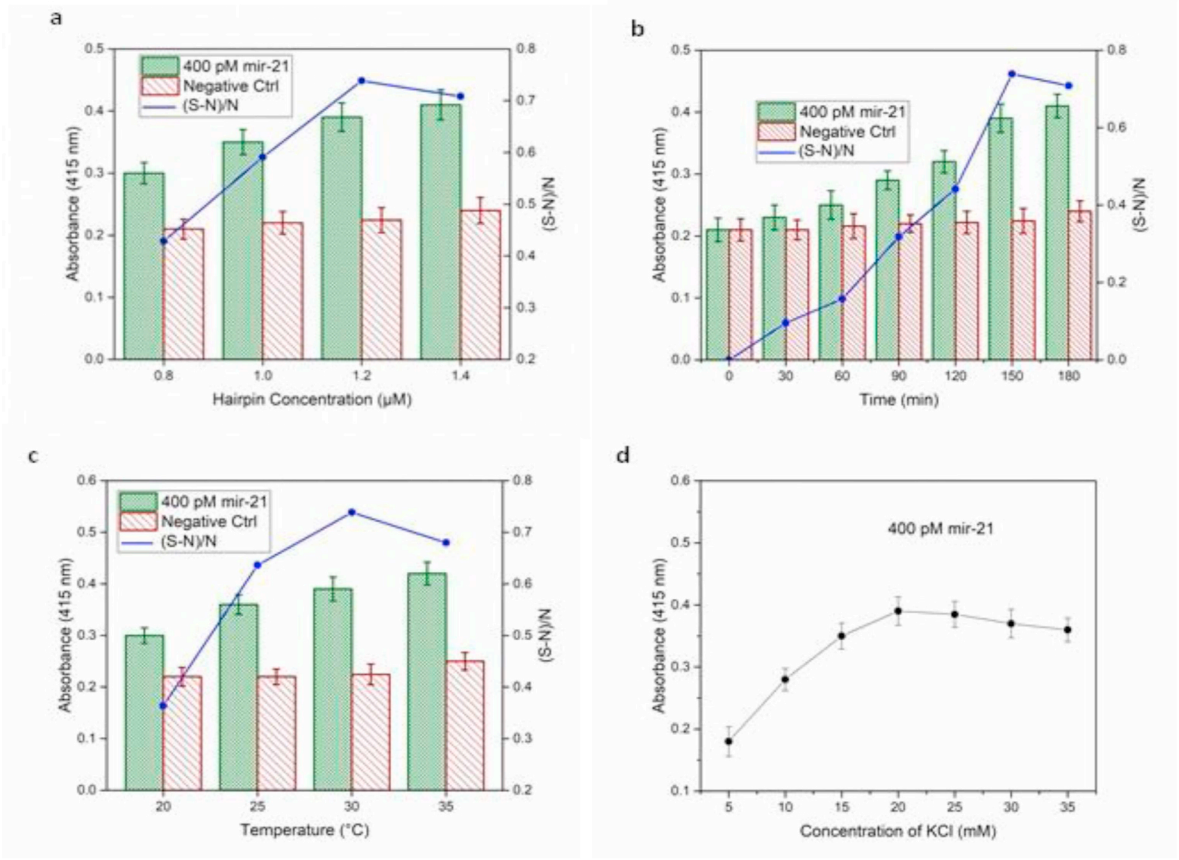

Fig. 3. Optimizations of experimental parameters. (a) Evaluation of the effect of hairpin concentration on nanodevice performance; (b) evaluation of the effect of the reaction incubation time on signal amplification; (c) evaluation of the effect of the reaction temperature on assay performance; and (d) optimizing KCl concentration for DNAzyme efficiency.

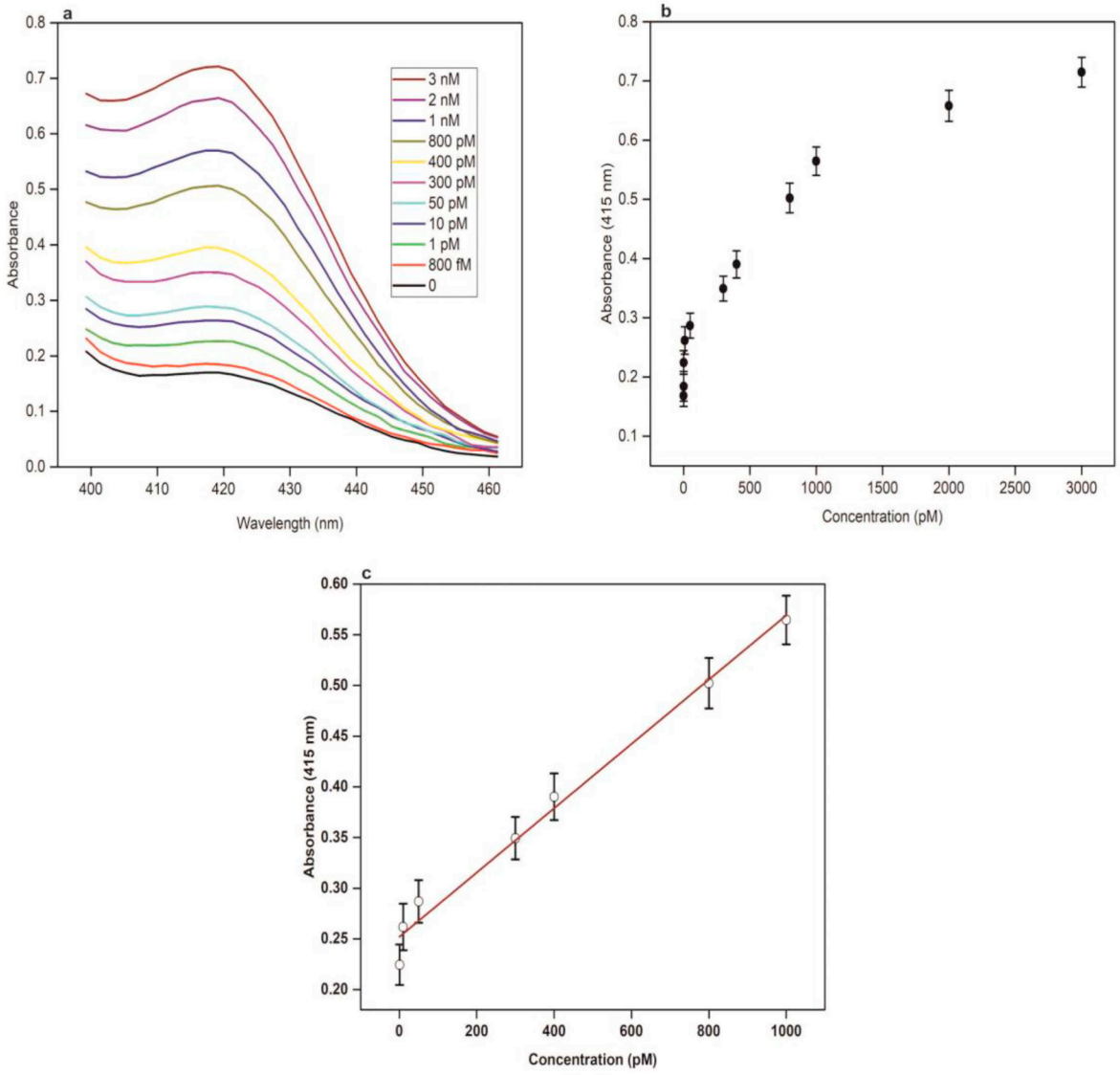

Fig. 4. Absorbance spectra upon addition of various concentrations of miR-21. (a) The curves from bottom to top correspond to the target miRNA with concentrations of 0, 800 fM, 1pM, 10 pM, 50 pM, 300 pM, 400 pM, 800 pM, 1 nM, 2 nM, 3 nM, respectively. (b) Calibration curve obtained from the absorbance values at 415 nm. (c) linear plot of the absorbance intensity vs. concentration of miR-21 over the range of 1 pM to 1 nM. Error bars are the standard deviations of three parallel experiments.

Table 2
Comparative analyses of b-HCR-based nanodevice and previous assays.

Ref	SBS[a]	Limitation	LOD[b]/Analyte	LR[c]
[25]	No evaluation quantitatively	Non-isothermal System leak, Non-efficient signal amplification	10 nM/DNA	–
[40]	32%	Complex, High cost	0.1 pM/DNA	0.1 pM–1 nM
[41]	No evaluation of SBS except for noncomplementary targets	Complex (fluorophore-DNAzyme), High cost	0.72 pM/ miRNA	1pM–10 nM
[26]	No evaluation of SBS	Complicated designs	0.1 nM/DNA	0.1nM-0.1 μM
[27]	60–65%	High cost (using PNA), Necessary to remove unreacted single-stranded DNAs, Non-linear amplification challenged	0.1 pM/DNA	0.1 pM- 10 nM
[23]	~13%	Expensive, System leak	0.5 pM/mRNA	1 pM–0.8 nM (quasi-linear)
[29]	37%	Complex	3 pM/miRNA	–
this study	52–54%	51–53%	Simple/Low cost	1 pM/miRNA	10pM – 1 nM

[a] Single base mismatch specificity.
[b] Limit of detection.
[c] Linear range.

by using the chemiluminescence resonance energy transfer (CRET) technology [41]. Moreover, Xuan et al. developed a dendrimer nanostructure to detect as low as 0.1 pM nucleic acids with a linearity of 0.1 p.m.–10 nM using an electrochemical approach [27]. Furthermore, Liu et al. designed a b-HCR system to detect 0.5 pM mRNA with a quasi-linear correlation of 1 pM to 0.8 nM [23]. In a similar work, Wie et al. recruited two HCR for constructing a hyper-branched nanostructure to detect miR-21, with a limit of detection of 3 pM [29]. Compared to above methods, our b-HCR assay amplifies chemical signal exponentially with comparable sensitivity to detect miR-21, Table 2.

Essentially, the enzyme-free approaches take place spontaneously under isothermal conditions that unlike enzymatic thermal cycler-dependent amplification methods like PCR [42] and LCR [43], which directly amplify the target molecule, indirectly amplify the target molecule [15,44]. In view of these characteristics and performing under different conditions, such as in a water bath, on the cell surface, or even inside living cells and also broad applications in synthetic biology and materials science, have encouraged the researchers to develop various isothermal, enzyme-free techniques for expanding (bio)analyte sensing [12,15]. In that line, HCR, in particular b-HCR, has been introduced recently to resolve some limitations like low sensitivity and specificity to develop ultrasensitive biosensors for various analytes detection [23,28,37]. Kinetically trapped isothermal b-HCR stays metastable in inactive form in the absence of target analyte, due to the closed structure of the hairpin monomers. However, in the presence of target molecule, the first HCR and the second HCR generate significantly amplified readout signal by synergistic effect to increase the sensitivity of our technique for accurate detection of the target miRNA. Indeed, in terms of the simplicity, cost, sensitivity, dynamic range and mismatch discrimination this strategy is comparable to the reported nonlinear HCR assays.

In spite of inferior performance in case of sensitivity compared with fluorescent assays, quencher to hairpins is expensive, ii) the attachment is not efficient, thereby probes may not be quenched perfectly in the absence of target molecule leading to high background signal, and iii) the fluorescence-based methods are intricate compared to our method. We think, the application of nanoparticle attached with linker and numerous initiators for b-HCR or engineering nanodevice to perform dendritically instead of b-HCR strategies could improve the assay sensitivity further.

3.6. Assay specificity

With the biological significance and crucial involvement in genetic variation by single nucleotide mutation, sequence-specific detection is a crucial issue to precise detection of defective molecule to evaluate disease situation or targeting the defective molecule. Besides, it is the most critical concern for any fabricated nanodevice to produce signal merely in the presence of specific stimulus. Distinguishing of miRNA family members with small size and with only a single different base is the biggest challenge of currently used nucleic acid-based methods. Methods with simple principle have poor mismatch discrimination ability [45,46], while complex enzyme-based methods with good functionality, selectivity and minute noise are tedious [47,48]. On this basis, specificity of the presented nanodevice was evaluated by detecting four different miRNA sequences, including a perfect target (miR-21), and three single-base mismatched molecules in the same position under identical conditions. As displayed in Fig. 5, signal induced by the perfect target clearly distinguished from the mismatched analogues with twice in concentration, no matter what type of the mutation accord, offering potential application to discriminate the target miRNA from mismatched analogues with only single base in difference. Although slight signal rise observed from 800 pM of inserted analogue, it is negligible compared to those of perfect molecule (miR-21) with 400 pM in concentration. Based on obtained result, present bottom-up assembling nanodevice with simple tool box showed high specificity for single mismatched analogue of miR-21.

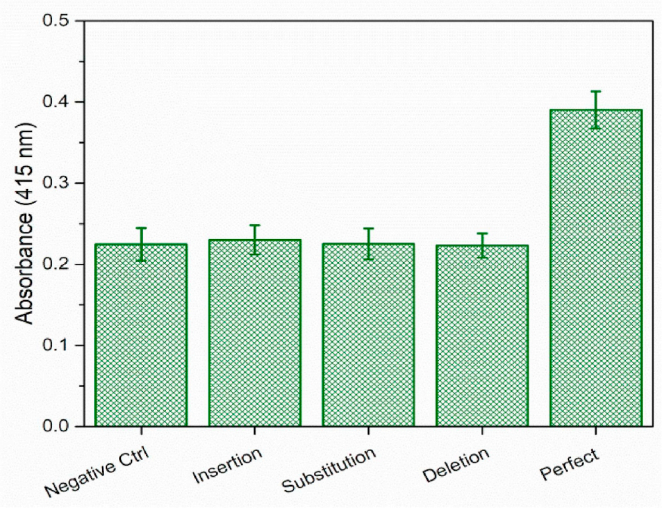

Fig. 5. Assay specificity of the DNA nanodevice toward 400 pM perfect target stimuli and 800p single-nucleotide mutations. Error bars are the standard deviations of three parallel experiments.

3.7. Application of the biosensor in real sample

To be useful in practical application and bioassays, any biosensor should be able to tolerate matrix effects of biological samples. Therefore, to demonstrate the practical application of the present nanodevice, various amounts of miR-21 (50, 400, 1000 pM) were spiked into 10% human serum (diluted with PBS buffer), to mimic the identical environment with real samples [49,50]. As seen in Fig. 6, responses obtained at 415 nm from the diluted serum were comparable to buffer samples. Similar to the buffer sample, the presence of 50 pM miR-21 in serum could be distinguished from the blank samples, which indicated that the analysis capability of the proposed nanodevice in complex mixtures was almost unaffected. Thus, the developed strategy may become a potential approach for visual detection of the miR-21 in complex biological samples.

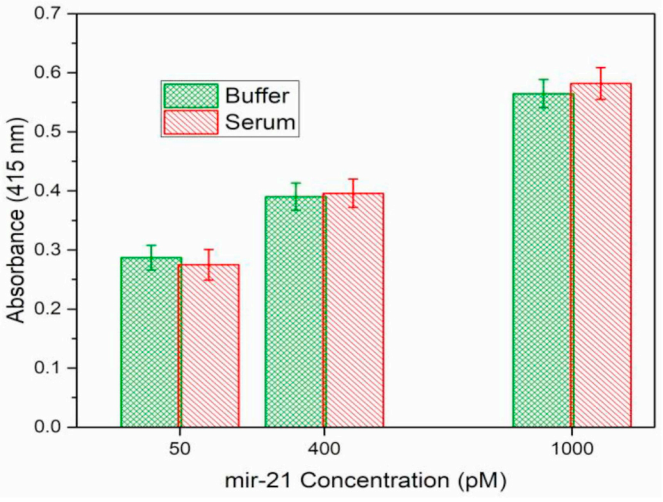

Fig. 6. Comparative data on the signal obtained by log concentration of different mir-21 inputs (50, 400, 1000 pM) in buffer and diluted serum samples. The error bars represent standard deviations of triplex measurements.

4. Conclusion

In summary a b-HCR approach was herein demonstrated to develop a versatile DNA nanodevice for miRNA detection. The working principle of b-HCR was a hierarchical coupling of two DNAzyme-coupled HCR circuits in a single reaction. Briefly, triggering the first HCR by the target miRNA activated the second HCR through split initiator segments embedded in the first HCR fuels (H_1 and H_2), resulting to branched nanowires. It's worthy to mention that this approach includes three signal amplification components: i) each nanowire acts as the conventional HCR and thus provides first unit of the signal amplification, ii) the branches which is derived from the conventional HCR are the second part of the signal amplification and, iii) the catalytic activity of the DNAzyme mediates the conversion of numerous substrate molecules to product repeatedly. In light of that, the proposed strategy can detect target miRNA as low as 1 pM with a three-decade linear range from 1 pM to 1 nM and can perfectly discriminate different single mismatches. Collectively, this bHCR strategy is a progressive achievement in various fields of nanotechnology which paves the routes toward obtaining elegant and more powerful nanodevices.

CRediT authorship contribution statement

Elyas Hosseinzadeh: Writing - original draft, Validation, Investigation, Project administration. **Hadi Ravan:** Conceptualization, Methodology, Software, Validation, Investigation, Resources, Data curation, Visualization, Writing - review & editing, Supervision, Project administration. **Abbas Mohammadi:** Funding acquisition. **Hossein Pourghadamyari:** Funding acquisition.

Declaration of competing interest

The authors declare that they have no known competing financial interests or personal relationships that could have appeared to influence the work reported in this paper.

Acknowledgments

This work was supported by Student Research Committee, Kerman University of Medical Sciences (Grant number: 97000025).

References

[1] B. Yurke, A.J. Turberfield, A.P. Mills Jr., F.C. Simmel, J.L. Neumann, A DNA-fuelled molecular machine made of DNA, Nature 406 (2000) 605.
[2] D.Y. Zhang, A.J. Turberfield, B. Yurke, E. Winfree, Engineering entropy-driven reactions and networks catalyzed by DNA, Science 318 (2007) 1121–1125.
[3] P. Yin, H.M.T. Choi, C.R. Calvert, N.A. Pierce, Programming biomolecular self-assembly pathways, Nature 451 (2008) 318–322.
[4] R.M. Dirks, N.A. Pierce, Triggered amplification by hybridization chain reaction, Proc. Natl. Acad. Sci. U. S. A 101 (2004) 15275–15278.
[5] S.F.J. Wickham, M. Endo, Y. Katsuda, K. Hidaka, J. Bath, H. Sugiyama, A.J. Turberfield, Direct observation of stepwise movement of a synthetic molecular transporter, Nat. Nanotechnol. 6 (2011) 166–169.
[6] D.Y. Zhang, G. Seelig, Dynamic DNA nanotechnology using strand-displacement reactions, Nat. Chem. 3 (2011) 103.
[7] G. Seelig, D. Soloveichik, D.Y. Zhang, E. Winfree, Enzyme-free nucleic acid logic circuits, Science 314 (2006) 1585–1588 80-.
[8] A. Phillips, L. Cardelli, A programming language for composable DNA circuits, J. R. Soc. Interface 6 (2009) S419–S436.
[9] P. Yin, H. Yan, X.G. Daniell, A.J. Turberfield, J.H. Reif, A unidirectional DNA walker that moves autonomously along a track, Angew. Chem. Int. Ed. 43 (2004) 4906–4911.
[10] Y. Kamiya, H. Asanuma, Light-driven DNA nanomachine with a photoresponsive molecular engine, Acc. Chem. Res. 47 (2014) 1663–1672.
[11] Y. Chen, M. Wang, C. Mao, An autonomous DNA nanomotor powered by a DNA enzyme, Angew. Chem. Int. Ed. 43 (2004) 3554–3557.
[12] F.C. Simmel, B. Yurke, H.R. Singh, Principles and applications of nucleic acid strand displacement reactions, Chem. Rev. 119 (2019) 6326–6369.
[13] E. Hosseinzadeh, H. Ravan, A. Mohammadi, R. Mohammad-rezaei, A. Norouzi, H. Hosseinzadeh, Target-triggered three-way junction in conjugation with catalytic concatemers-functionalized nanocomposites provides a highly sensitive colorimetric method for miR-21 detection, Biosens. Bioelectron. 117 (2018) 567–574.
[14] Z. Cheglakov, T.M. Cronin, C. He, Y. Weizmann, Live cell microRNA imaging using cascade hybridization reaction, J. Am. Chem. Soc. 137 (2015) 6116–6119.
[15] Y. Zhao, F. Chen, Q. Li, L. Wang, C. Fan, Isothermal amplification of nucleic acids, Chem. Rev. 115 (2015) 12491–12545.
[16] F. Wang, J. Elbaz, R. Orbach, N. Magen, I. Willner, Amplified analysis of DNA by the autonomous assembly of polymers consisting of DNAzyme wires, J. Am. Chem. Soc. 133 (2011) 17149–17151.
[17] J. Dong, X. Cui, Y. Deng, Z. Tang, Amplified detection of nucleic acid by G-quadruplex based hybridization chain reaction, Biosens. Bioelectron. 38 (2012) 258–263.
[18] H.M.T. Choi, V.A. Beck, N.A. Pierce, Next-generation in situ hybridization chain reaction: higher gain, lower cost, greater durability, ACS Nano 8 (2014) 4284–4294.
[19] L. Yang, C. Liu, W. Ren, Z. Li, Graphene surface-anchored fluorescence sensor for sensitive detection of microRNA coupled with enzyme-free signal amplification of hybridization chain reaction, ACS Appl. Mater. Interfaces 4 (2012) 6450–6453.
[20] Y. Liao, Y. Fu, Y. Wu, R. Huang, X. Zhou, D. Xing, Ultrasensitive detection of MicroRNA in tumor cells and tissues via continuous assembly of DNA probe, Biomacromolecules 16 (2015) 3543–3551.
[21] Y. Zhang, Z. Chen, Y. Tao, Z. Wang, J. Ren, X. Qu, Hybridization chain reaction engineered dsDNA for Cu metallization: an enzyme-free platform for amplified detection of cancer cells and microRNAs, Chem. Commun. 51 (2015) 11496–11499.
[22] A. Norouzi, H. Ravan, A. Mohammadi, E. Hosseinzadeh, M. Norouzi, T. Fozooni, Aptamer–integrated DNA nanoassembly: a simple and sensitive DNA framework to detect cancer cells, Anal. Chim. Acta 1017 (2018) 26–33.
[23] L. Liu, J.-W. Liu, H. Wu, X.-N. Wang, R.-Q. Yu, J.-H. Jiang, Branched hybridization chain reaction (bHCR) circuit for ultrasensitive localizable imaging of mRNA in living cells, Anal. Chem. 90 (2018) 1502–1505.
[24] F. Wang, C.-H. Lu, I. Willner, From cascaded catalytic nucleic acids to enzyme–DNA nanostructures: controlling reactivity, sensing, logic operations, and assembly of complex structures, Chem. Rev. 114 (2014) 2881–2941.
[25] H. Chandran, A. Rangnekar, G. Shetty, E.A. Schultes, J.H. Reif, T.H. LaBean, An autonomously self-assembling dendritic DNA nanostructure for target DNA detection, Biotechnol. J. 8 (2013) 221–227.
[26] F. Xuan, I.-M. Hsing, Triggering hairpin-free chain-branching growth of fluorescent DNA dendrimers for nonlinear hybridization chain reaction, J. Am. Chem. Soc. 136 (2014) 9810–9813.
[27] F. Xuan, T.W. Fan, I.-M. Hsing, Electrochemical interrogation of kinetically-controlled dendritic DNA/PNA assembly for immobilization-free and enzyme-free nucleic acids sensing, ACS Nano 9 (2015) 5027–5033.
[28] Y. Tang, X.-L. Zhang, L.-J. Tang, R.-Q. Yu, J.-H. Jiang, In situ imaging of individual mRNA mutation in single cells using ligation-mediated branched hybridization chain reaction (ligation-bHCR), Anal. Chem. 89 (2017) 3445–3451.
[29] J. Wei, X. Gong, Q. Wang, M. Pan, X. Liu, J. Liu, F. Xia, F. Wang, Construction of an autonomously concatenated hybridization chain reaction for signal amplification and intracellular imaging, Chem. Sci. 9 (2018) 52–61.
[30] X. Wang, A PCR-based platform for microRNA expression profiling studies, RNA 15 (2009) 716–723.
[31] M.Y. Shah, G.A. Calin, MicroRNAs as therapeutic targets in human cancers, Wiley Interdiscip. Rev. RNA. 5 (2014) 537–548.
[32] J.M. Picuri, B.M. Frezza, M.R. Ghadiri, Universal translators for nucleic acid diagnosis, J. Am. Chem. Soc. 131 (2009) 9368–9377.
[33] H. Ravan, Translating nucleic-acid hybridization into universal DNA-reporter sequences, TrAC Trends Anal. Chem. (Reference Ed.) 65 (2015) 97–106.
[34] H. Ravan, Implementing a two-layer feed-forward catalytic DNA circuit for enzyme-free and colorimetric detection of nucleic acids, Anal. Chim. Acta 910 (2016) 68–74.
[35] Y. Zhang, Y. Yan, W. Chen, W. Cheng, S. Li, X. Ding, D. Li, H. Wang, H. Ju, S. Ding, A simple electrochemical biosensor for highly sensitive and specific detection of microRNA based on mismatched catalytic hairpin assembly, Biosens. Bioelectron. 68 (2015) 343–349.
[36] Y.S. Jiang, S. Bhadra, B. Li, A.D. Ellington, Mismatches improve the performance of strand-displacement nucleic acid circuits, Angew. Chem. Int. Ed. 53 (2014) 1845–1848.
[37] X. Chen, N. Briggs, J.R. McLain, A.D. Ellington, Stacking nonenzymatic circuits for high signal gain, Proc. Natl. Acad. Sci. Unit. States Am. 110 (2013) 5386–5391.
[38] Y. Li, D. Sen, Toward an efficient DNAzyme, Biochemistry 36 (1997) 5589–5599.
[39] P. Travascio, Y. Li, D. Sen, DNA-enhanced peroxidase activity of a DNA aptamer-hemin complex, Chem. Biol. 5 (1998) 505–517.
[40] S. Bi, M. Chen, X. Jia, Y. Dong, Z. Wang, Hyperbranched hybridization chain reaction for triggered signal amplification and concatenated logic circuits, Angew. Chem. Int. Ed. 54 (2015) 8144–8148.
[41] S. Bi, S. Yue, Q. Wu, J. Ye, Triggered and catalyzed self-assembly of hyperbranched DNA structures for logic operations and homogeneous CRET biosensing of microRNA, Chem. Commun. 52 (2016) 5455–5458.
[42] K.B. Mullis, F.A. Faloona, Specific synthesis of DNA in vitro via a polymerase-catalyzed chain reaction, Recomb. DNA Methodol. Elsevier, 1989, pp. 189–204.
[43] F. Barany, Genetic disease detection and DNA amplification using cloned thermostable ligase, Proc. Natl. Acad. Sci. Unit. States Am. 88 (1991) 189–193.
[44] H. Ravan, M. Amandadi, S. Esmaeili-Mahani, DNA domino-based nanoscale logic circuit: a versatile strategy for ultrasensitive multiplexed analysis of nucleic acids, Anal. Chem. 89 (2017) 6021–6028.
[45] M.B. Baker, G. Bao, C.D. Searles, In vitro quantification of specific microRNA using molecular beacons, Nucleic Acids Res. 40 (2011) e13–e13.

[46] J. Xu, H. Dong, W. Shen, S. He, H. Li, Y. Lu, Z.-S. Wu, L. Jia, New molecular beacon for p53 gene point mutation and significant potential in serving as the polymerization primer, Biosens. Bioelectron. 66 (2015) 504–511.
[47] Y. Cheng, X. Zhang, Z. Li, X. Jiao, Y. Wang, Y. Zhang, Highly sensitive determination of microRNA using target-primed and branched rolling-circle amplification, Angew. Chem. Int. Ed. 48 (2009) 3268–3272.
[48] R. Deng, L. Tang, Q. Tian, Y. Wang, L. Lin, J. Li, Toehold-initiated rolling circle amplification for visualizing individual microRNAs in situ in single cells, Angew, Chemie Int. Ed. 53 (2014) 2389–2393.
[49] K.-J. Huang, Y.-J. Liu, H.-B. Wang, Y.-Y. Wang, Y.-M. Liu, Sub-femtomolar DNA detection based on layered molybdenum disulfide/multi-walled carbon nanotube composites, Au nanoparticle and enzyme multiple signal amplification, Biosens. Bioelectron. 55 (2014) 195–202.
[50] W. Zhou, X. Gong, Y. Xiang, R. Yuan, Y. Chai, Quadratic recycling amplification for label-free and sensitive visual detection of HIV DNA, Biosens. Bioelectron. 55 (2014) 220–224.